DOI: 10.1002/cjoc.201400003

High-Performance Cobalt Selenide and Nickel Selenide Nanocomposite Counter Electrode for Both Iodide/Triiodide and Cobalt(II/III) Redox Couples in Dye-Sensitized Solar Cells

Zaiwei Wang,[a,b,†] Hongxia Xu,[a,†] Zhongyi Zhang,[a] Xinhong Zhou,*[,c] Shuping Pang,[a] and Guanglei Cui*[,a]

[a] *Qingdao Key Lab of Solar Energy Utilization and Energy Storage Technology, Qingdao Institute of Bioenergy and Bioprocess Technology, Chinese Academy of Sciences, Qingdao, Shandong 266101, China*
[b] *University of Chinese Academy of Sciences, Beijing 100080, China*
[c] *Qingdao University of Science and Technology, Qingdao, Shandong 266101, China*

The nanocomposites of cobalt selenide and nickel selenide ($Co_{0.85}Se/Ni_{0.85}Se$) were successfully fabricated on FTO glass by a facile co-electrodeposition method at ambient temperature. Nanocomposite films were used as electrocatalysts in dye-sensitized solar cell counter electrodes for regeneration of both iodide/triiodide and cobalt(II/III) redox couples. $Co_{0.85}Se/Ni_{0.85}Se$ were mainly composed of nanoflakes and nanoparticles. It is noted that such nanostructure generated by nanoparticles embedded with 2D nanoflakes led to high active sites and was accessible to cobalt(II/III) electrolyte, delivering better catalytic activity for the reduction of larger volume cobalt(II/III). As a result, for cobalt(II/III) electrolyte, the $Co_{0.85}Se/Ni_{0.85}Se$ based dye-sensitized solar cell performed significantly improved efficiency than that of Pt and $Co_{0.85}Se$. Meanwhile, the $Co_{0.85}Se/Ni_{0.85}Se$ based dye-sensitized solar cell held comparable energy conversion efficiency to that of Pt and $Co_{0.85}Se$ for iodide/triiodide electrolyte.

Keywords counter electrode, dye-sensitized solar cells, iodide/triiodide, cobalt(II/III), metal selenide

Introduction

Dye-sensitized solar cells (DSSCs), introduced by Grätzel and O'Regan in 1991, have attracted much attention due to low cost, ease of fabrication and comparable high efficiency.[1-6] Typically, a DSSC consists of a dye-sensitized nanocrystalline TiO_2 semiconductor electrode, a counter electrode (CE), and an electrolyte containing a redox couple. The redox couple in the electrolyte regenerates the dye on photoanode back to ground state and is reduced at counter electrode. The open-circuit voltage (V_{oc}) of a dye-sensitized solar cell is defined as the absolute difference between the standard reduction potential of redox couple and the Fermi level of the TiO_2 photoelectrode.[7,8] Therefore, the redox couples and the counter electrode materials are very important to minimize the energy losses and increase the V_{oc}. To date, the I_3^-/I^- redox electrolyte has been almost exclusively utilized in DSSCs. However, the I_3^-/I^- redox electrolyte has several critical disadvantages such as the corrosion of copper/silver lines, visible light absorption and the complicated redox chemistry to cause great energy loss.[9-11] To overcome these limitations, new redox couples including TEMPO/TEMPO$^+$,[12] TMTU/TMFDS^{2+},[13] thiolate/disulfide,[14] ferrocene(0/+),[15] copper(I/II),[16-18] and cobalt(II/III)[19-24] were explored. Recently, major progress has been achieved through the development of DSSCs based on electrolyte containing cobalt(II/III) redox couple, which afford record efficency of up to 12.3%.[24]

Typically, the noble metal platinum is used as the counter electrodes in DSSCs. However, as a noble metal, platinum is scarce and expensive which may hinder the potential large scale applications. Therefore, it is highly imperative to explore low-cost, abundant, and highly efficient substitutes for the conventional Pt counter electrode in the DSSC system. In recent years, several kinds of fascinating materials such as carbonaceous materials,[5,25-28] conductive polymer[29,30] and metal compounds (metal nitrides,[31-33] metal carbides,[34,35] metal sulfides,[36-39] metal selenides[40,41] and metal telluride[42]) were extensively investigated as counter electrodes for DSSCs. These substitutes showed comparable catalytic activity for I_3^-/I^-. However, these substitutes are always not effective for improving the catalytic activity of CEs for DSSCs containing cobalt(II/III). This is

* E-mail: cuigl@qibebt.ac.cn; Tel.: 0086-0532-80662746; Fax: 0086-0532-80662744
Received January 1, 2014; accepted March 27, 2014; published online April 22, 2014.
Supporting information for this article is available on the WWW under http://dx.doi.org/10.1002/cjoc.201400003 or from the author.
† These authors contributed equally to this work.

because the volume of cobalt(II/III) complexes is larger than that of I_3^-/I^-. It is difficult to access to catalytic active sites with smaller space volume for cobalt redox couples. Therefore, it is of great significance to further explore the catalytic activity by rational design and facile synthesis of nanostructured catalysts materials.

It is reported that metal selenides, due to their unique electronic configuration and comparatively high catalytic activity, presented superior catalytic activity for the triiodide reduction. Wang *et al.*[40] prepared metal selenides ($Co_{0.85}Se$ and $Ni_{0.85}Se$) on conductive glass substrates through a hydrothermal method at high temperature in an autoclave and presented the highest PCE for I_3^-/I^- with as-prepared metal selenides counter electrode. Cui *et al.*[41a] reported that nanostructured cobalt selenide with honeycomb-like morphology by a facile electrodeposition method exhibited superior catalytic activity for the triiodide reduction. To the best of our knowledge, no research on metal selenides for use in DSSCs for cobalt(III) reduction has been reported so far. In this paper, cobalt selenide/nickel selenide ($Co_{0.85}Se$/$Ni_{0.85}Se$) nanocomposite films were designed to improve catalytic activity for cobalt(II/II) redox couples. $Co_{0.85}Se/Ni_{0.85}Se$ nanocomposite films were fabricated on FTO substrate at ambient temperature by an co-electrodeposition method. It was demonstrated that $Co_{0.85}Se/Ni_{0.85}Se$ nanocomposite films displayed comparable catalytic activity for the iodide/tiriodide redox couples with $Co_{0.85}Se$ films and Pt films, moreover, presented better catalytic activity than $Co_{0.85}Se$ films and Pt films for cobalt(II/III) redox couples.

Experimental

Preparation of $Co_{0.85}Se$, $Co_{0.85}Se/Ni_{0.85}Se$ and Pt-FTO CEs

$Co_{0.85}Se$ films and $Co_{0.85}Se/Ni_{0.85}Se$ nanocomposite films were prepared by an electrodeposition method, as described by Zhang *et al.*[41a] The deposition bath of $Co_{0.85}Se$ was a 50 mL aqueous solution containing 20 mmol/L Na_2SeO_3, 20 mmol/L $Co(CH_3COO)_2$ and 100 mmol/L LiCl. The deposition bath of $Co_{0.85}Se/Ni_{0.85}Se$ nanocomposite was a 50 mL aqueous solution containing 20 mmol/L Na_2SeO_3, 10 mmol/L $Co(CH_3COO)_2$, 10 mmol/L $Ni(CH_3COO)_2$ and 100 mmol/L LiCl. The pH values of the solutions were controlled to 3.5 adjusted with HCl. The deposition was conducted at room temperature in a single compartment glass cell with three-electrode configuration using a CHI 660D electrochemical workstation (CH Instruments). The FTO substrate was previously cleaned with detergent and de-ionized water, followed by sonication in isopropanol for three times. A Pt foil and Ag/AgCl electrode were used as auxiliary electrode and reference electrode, respectively. The potentiostatic electrodeposition technology was used, for which the deposition potential was maintained at −0.8 V versus Ag/AgCl electrode and the deposition time was 30 s. Finally, the FTO glass was washed with de-ionized water and dried in an air flow. The mirror-like Pt-FTO electrode was obtained by electrodepositing a platinum layer on the surface of fluorine-doped tin oxide substrate. The thickness of Pt films is about 75 nm.

Fabrication of DSSC devices

TiO_2 working photoanodes were prepared on FTO substrate using TiO_2 paste by doctor blade technique and subsequently sintered at 500 ℃ for 30 min in air. The resultant TiO_2 photoanodes were respectively soaked in an ethanol solution of N719 dye (3×10^{-4} mol/L) for I_3^-/I^- electrolyte or Z907 dye (3×10^{-4} mol/L) for cobalt(II/III) electrolyte for 24 h to obtain dye-sensitized TiO_2 electrodes. Two kinds of electrolytes were used in this paper. The first is the I_3^-/I^- electrolyte which contains 0.6 mol/L 1,2-dimethyl-3-propylimidazolium iodide (DMPII), 0.03 mol/L iodine (I_2), 0.06 mol/L lithium iodide (LiI), 0.5 mol/L 4-*tert*-butylpyridine (TBP), and 0.1 mol/L guanidinium thiocyannate with acetonitrile (ACN) as the solvent. The second is cobalt(II/III) electrolyte which is composed of 0.22 mol/L $[Co^{II}(Me_2bpy)_3](PF_6)_2$, 0.055 mol/L $[Co^{III}(Me_2bpy)_3](PF_6)_3$, 0.2 mol/L 4-*tert*-butylpyridine (TBP) and 0.1 mol/L LiTFSI in acetonitrile. The cobalt redox couple was synthesized by the literature method.[43] The DSSC for iodide redox couple was assembled with the N719 dye adsorbed TiO_2 photoanode and counter electrodes sandwiching the iodide redox couple electrolyte and sealed by insulating tape. Meanwhile, the DSSC for cobalt complex redox couple was assembled with the Z907 dye adsorbed TiO_2 photoanode and counter electrodes sandwiching the cobalt complex redox couple electrolyte and sealed by insulating tape.

Characterizations

Scanning electron microscope (SEM) images were acquired using a Hitachi S-4800 field emission electron microscope. Scanning transmission electron microscope (STEM) and energy dispersive X-ray spectroscopy (EDS) were obtained from Tecnai F20. X-ray diffraction (XRD) patterns were recorded with a Bruker-AXS Microdiffractometer (D8 ADVANCE) using Cu Kα radiation (λ=1.5406 Å) from 5° to 95°. Cyclic voltammetry (CV) was carried out in a three-electrode system in an acetonitrile solution of 0.1 mol/L $LiClO_4$, 10 mmol/L LiI, and 1 mmol/L I_2. Platinum served as a counter electrode and the nonaqueous Ag/Ag^+ couple was used as a reference electrode. The photocurrent-voltage characteristics of the DSSCs were measured with a Newport (USA) solar simulator (300 W Xe source) and a Keithley 2420 source meter. Electrochemical impedance spectroscopy (EIS) measurements were performed using a Zahner Ennium electrochemical workstation by applying an AC voltage of 10 mV amplitude in the frequency range between 100 kHz and 100 mHz at room temperature.

CHINESE JOURNAL OF CHEMISTRY

Results and Discussion

Characterization of the as-synthesized metal selenides films

Typical SEM images of as-synthesized cobalt selenide and cobalt selenide/nickel selenide nanocomposite are shown in Figure 1. It can be seen that the electrodeposited metal selenide possessed a high uniformity. As shown in Figure 1(a), cobalt selenide film had a honeycomb-like structure formed by sheets intersected together which was consistent to the recent report.[41a] When nickel was introduced, as shown in Figure 1(b), the cobalt selenide/nickel selenide nanocomposite film exhibited a morphology of nanoparticles embedded with 2D nanoflakes. Meantime, nanoparticles with the diameters of about 150 nm are interconnected by nanoflakes which is beneficial to improving electrical conductivity. The XRD patterns of the electrodeposited metal selenides are shown in Figure 2. The peaks of cobalt selenide can be well indexed to $Co_{0.85}Se$ (JCPDS No. 52-1008). The diffraction peaks of cobalt selenide/nickel selenide nanocomposite were very consistent with those of $Co_{0.85}Se$ (JCPDS No. 52-1008) or $Ni_{0.85}Se$ (JCPDS No. 18-0888) because of their structural similarity. Scanning transmission electron microscopy (STEM) image and the corresponding energy-dispersive X-ray spectroscopy (EDS) (Figure 1S) were performed to determine the local composition of the $Co_{0.85}Se/Ni_{0.85}Se$ nanocomposite. As shown in Figure 1Sa, nanoflakes exhibited almost the signals of both cobalt and selenium, while cobalt, nickel and selenium signals are homogeneously distributed throughout the nanoparticle. Combining the XRD results and EDS measurement, we deduced that $Co_{0.85}Se/Ni_{0.85}Se$ were mainly composed of $Co_{0.85}Se$ nanoflakes and $Ni_{0.85}Se$ nanoparticles.

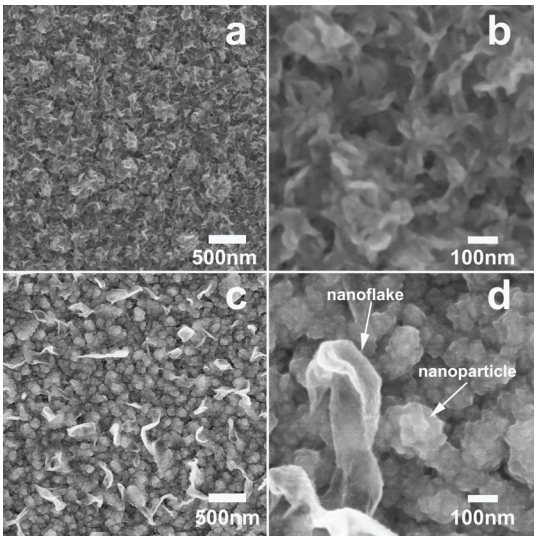

Figure 1 Typical SEM images of $Co_{0.85}Se$ (a, b) and $Co_{0.85}Se/Ni_{0.85}Se$ (c, d).

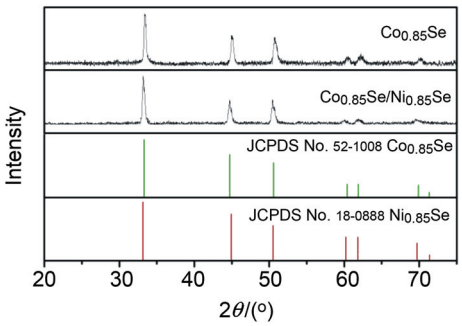

Figure 2 XRD patterns of $Co_{0.85}Se$ and $Co_{0.85}Se/Ni_{0.85}Se$.

Photovoltaic performance of iodide/triiodide based DSSCs using $Co_{0.85}Se/Ni_{0.85}Se$ counter electrode

In the present study, we first investigated electrocatalytic activity of $Co_{0.85}Se/Ni_{0.85}Se$ nanocomposite films for iodide/triiodide redox couple by cyclic voltammetry (CV) (Figure 3). The CV curves of $Co_{0.85}Se$ and Pt counter electrodes are also presented for a fair comparison. The cyclic voltammetry (CV) results demonstrated that all of the materials showed two redox peaks, which suggested that all of these materials possessed good catalytic performance for iodide/triiodide redox couples. The relative negative pair is assigned to the redox reaction (Eq. 1) and the positive pair is ascribed to redox reaction (Eq. 2).[44]

$$I_3^- + 2e^- \rightleftharpoons 3I^- \quad (1)$$

$$3I_2 + 2e^- \rightleftharpoons 2I_3^- \quad (2)$$

The peak currents and cathodic peak potentials are two important parameters for evaluating catalytic activities of different CEs.[45] The relative negative redox peaks show a direct effect on the performance of DSSCs. Therefore, we focused on investigation about peak current density and cathodic peak potentials of the relative negative redox peaks. $Co_{0.85}Se$ and $Co_{0.85}Se/Ni_{0.85}Se$ had similar cathodic peak potentials which were slightly positive than that of Pt-FTO, indicating a lower overpotential for reduction of I_3^- to I^-. This result demonstrated $Co_{0.85}Se$ and $Co_{0.85}Se/Ni_{0.85}Se$ possessed better alleviated polarization of the redox reaction than that of Pt-FTO. The cathodic current densities of $Co_{0.85}Se$ and $Co_{0.85}Se/Ni_{0.85}Se$ were larger than that of Pt-FTO. These revealed that $Co_{0.85}Se$ and $Co_{0.85}Se/Ni_{0.85}Se$ exhibited better I_3^-/I^- catalytic performance than that of Pt-FTO. $Co_{0.85}Se/Ni_{0.85}Se$ presented similar cathodic peak potentials but slightly smaller cathodic current density than that of $Co_{0.85}Se$, demonstrating $Co_{0.85}Se/Ni_{0.85}Se$ nanocomposites film possessed fair electrocatalytic activity with $Co_{0.85}Se$ for iodide/triiodide redox couples. Compared with the Pt CE, these two metal selenides CEs exhibited more positive cathodic peak potentials and larger cathodic peak current density. Thus, in terms of I_3^-/I^- redox reaction, it can be concluded that both the

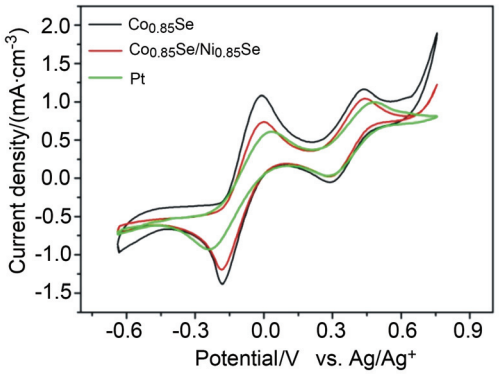

Figure 3 Cyclic voltammograms of Pt, $Co_{0.85}Se$ and $Co_{0.85}Se/Ni_{0.85}Se$ counter electrodes in 10 mmol/L LiI, 1 mmol/L I_2 and 0.1 mol/L $LiClO_4$ acetonitrile solution at a scan rate of 20 mV•s^{-1}.

electrocatalytic activity and the reversibility of the metal selenide CEs are better than the conventional Pt CE.

To further investigate the charge transfer process and evaluate the catalytic activities of various CEs in the reduction of I_3^-, electrochemical impedance spectra (EIS) of the samples were measured using symmetric cells fabricated with two identical electrodes. Nyquist plots of symmetric cells with different electrodes are illustrated in Figure 4, in which two semicircles are observed in the high and low frequency regions. According to electrochemical process for reduction of iodide, the semicircle in the high frequency region corresponds to the charge transfer resistance of counter electrode/redox (I_3^-/I^-) interface (R_{ct}) and the capacitance of the counter electrode/electrolyte interface. The low-frequence semicircle is attributed to the Nernst diffusion impedance of the I_3^-/I^- redox species within a thin layer in the electrolyte.[46] The high-frequency intercept on the real axis represents the series resistance (R_s), including the sheet resistance of two identical electrodes and the electrolytic resistance. The equivalent circuit used is given in Figure S2 and the simulated data from the EIS spectra are summarized in Table 1.

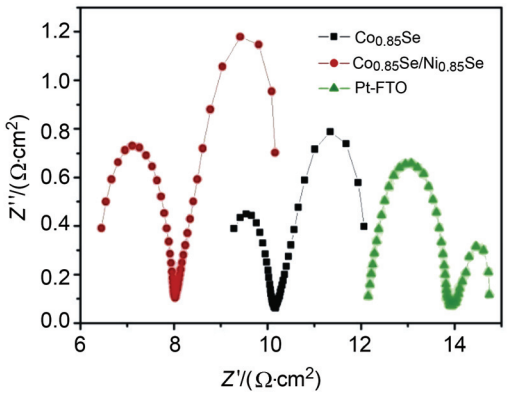

Figure 4 Nyquist plots for symmetric cells fabricated with two identical counter electrode of Pt, $Co_{0.85}Se$ and $Co_{0.85}Se/Ni_{0.85}Se$ filled with I_3^-/I^- electrolyte. The cells were measured in the frequency range between 100 kHz and 100 mHz.

The R_s value of $Co_{0.85}Se/Ni_{0.85}Se$ composite film electrodes was lower than that of $Co_{0.85}Se$. This demonstrated $Ni_{0.85}Se$ had the robust bonding with FTO than $Co_{0.85}Se$, which is consistent with the previous report.[40] The simulated charge transfer resistances of $Co_{0.85}Se$, $Co_{0.85}Se/Ni_{0.85}Se$ and Pt-FTO counter electrode are 0.93 1.55, and 1.14 Ω•cm^2, respectively. The smaller R_{ct} for $Co_{0.85}Se$ and $Co_{0.85}Se/Ni_{0.85}Se$ implied that they had better catalytic activities on the reduction of triiodide and comparable to the expensive Pt as the CE in DSSCs. However, $Co_{0.85}Se/Ni_{0.85}Se$ is slightly inferior to $Co_{0.85}Se$ for catalyzing the reduction of I_3^- due to inferior catalytic activity of $Ni_{0.85}Se$ compared with Pt and $Co_{0.85}Se$, which is consistent with the previous report.[40] The conclusions for the catalytic activity derived from the EIS are consistent with CV data.

Table 1 EIS parameters of the symmetric cells based on different counter electrodes filled with different electrolyte

Counter electrode	R_s^a/(Ω•cm^2)	R_{ct}^a/(Ω•cm^2)[a]	R_s^b/(Ω•cm^2)	R_{ct}^b/(Ω•cm^2)
$Co_{0.85}Se$	9.20	0.93	7.56	31.92
$Co_{0.85}Se/Ni_{0.85}Se$	6.42	1.55	7.13	7.39
Pt-FTO	12.26	1.14	8.52	76.46

[a] Filled with I_3^-/I^- electrolyte; [b] filled with Co(II/III) electrolyte.

The photocurrent density-voltage (*J-V*) characteristic curves of the DSSCs fabricated with different counter electrodes in I_3^-/I^- electrolyte measured under the illumination of 1 sun (100 mW•cm^{-2}) are shown in Figure 5. The photovoltaic parameters of these devices, including the short-circuit current (J_{sc}), the open-circuit voltage (V_{oc}), the fill factor (FF), and the energy conversion efficiency (η), are summarized in Table 2. The DSSCs based $Co_{0.85}Se$, $Co_{0.85}Se/Ni_{0.85}Se$ and Pt CEs yield PEC of 8.45% (V_{oc}=772 mV, J_{sc}=16.27 mA/cm^2, FF=67.27%), 8.12% (V_{oc}=777 mV, J_{sc}=15.66 mA/cm^2, FF=66.66%), and 8.03% (V_{oc}=797 mV, J_{sc}=15.65 mA/cm^2, FF=64.38%), respectively. It is obvious that $Co_{0.85}Se$ and $Co_{0.85}Se/Ni_{0.85}Se$-based DSSCs showed slightly larger photocurrent density and fill factor than that of conventional Pt CEs. The slightly improvement can be mainly ascribed to a more efficient electrochemical catalytic activity of metal selenides. $Co_{0.85}Se/Ni_{0.85}Se$-based DSSCs produced a slightly lower PCE than that of $Co_{0.85}Se$ CE which is in good accordance with the CV and EIS. The results of CV,

Table 2 Photovoltaic parameters of the DSSCs using different kinds of CE and I_3^-/I^- electrolyte

Counter electrode	V_{oc}/mV	J_{sc}/(mA•cm^{-2})	FF/%	η/%
$Co_{0.85}Se$	772	16.27	67.27	8.45
$Co_{0.85}Se/Ni_{0.85}Se$	777	15.66	66.66	8.12
Pt-FTO	797	15.65	64.38	8.03

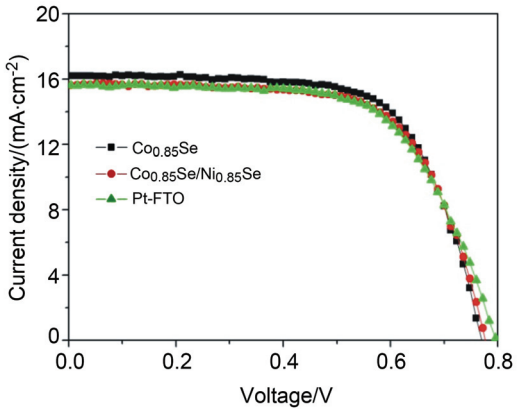

Figure 5 Characteristic photocurrent density-voltage (*J-V*) curves of DSSCs with different electrodes, measured under simulated sunlight 100 mW•cm^{-2} (AM 1.5). The liquid electrolyte is composed of 0.6 mol/L 1,2-dimethyl-3-propylimidazolium iodide (DMPII), 0.03 mol/L iodine (I_2), 0.06 mol/L lithium iodide (LiI), 0.5 mol/L 4-*tert*-butylpyridine (TBP), and 0.1 mol/L guanidinium thiocyannate in acetonitrile solution.

EIS and the photovoltaic performance demonstrated that $Co_{0.85}Se/Ni_{0.85}Se$ possessed almost comparable electrocatalytic activity for reduction of I_3^- with $Co_{0.85}Se$.

Photovoltaic performance of Co(II)/Co(III) electrolyte based DSSCs using $Co_{0.85}Se/Ni_{0.85}Se$ counter electrode

To date, the highest energy conversion efficiency (12.3%) has been obtained through the development of DSSCs based on electrolyte containing Co(II)/Co(III) redox couple. It is highly imperative to explore low cost, highly efficient catalyst for the reduction of Co(III). However, the volume of cobalt complexes is larger which limited the charge transfer rate and mass transport of the cobalt redox couple in the electrolyte. Therefore, it is necessary to rationally design nanostructured catalyst which delivers the Co(III) complex accessible to catalytic active sites.

In this paper, $Co_{0.85}Se/Ni_{0.85}Se$, $Co_{0.85}Se$ and Pt were used for reduction of Co(III). The photocurrent density-voltage (*J-V*) characteristic curves of the DSSCs fabricated with different counter electrodes in Co(II/III) electrolyte measured under the illumination of 1 sun (100 mW•cm^{-2}) are shown in Figure 6. The photovoltaic parameters of these devices, including the short-circuit current (J_{sc}), the open-circuit voltage (V_{oc}), the fill factor (FF), and the energy conversion efficiency (η), are summarized in Table 3. The DSSCs using $Co_{0.85}Se$, $Co_{0.85}Se/Ni_{0.85}Se$ and Pt-FTO CEs for cobalt complex electrolyte show PCEs of 1.57%, 2.54%, and 1.74%, respectively. $Co_{0.85}Se$ presented a comparable catalytic activity for the reduction of the cobalt complex electrolyte with Pt. Nevertheless, the DSSC using the $Co_{0.85}Se/Ni_{0.85}Se$ CE yielded a best PCE, an improvement of 46% compared with the Pt-based DSSC. It is worth noting that $Co_{0.85}Se/Ni_{0.85}Se$ is more efficient for the reduction of the cobalt complex electrolyte than

Table 3 Photovoltaic parameters of the DSSCs using different kinds of CE and Co(II/III) electrolyte

Counter electrode	V_{oc}/mV	J_{sc}/(mA•cm^{-2})	FF/%	η/%
$Co_{0.85}Se$	443	7.82	45.47	1.57
$Co_{0.85}Se/Ni_{0.85}Se$	651	7.37	52.96	2.54
Pt-FTO	578	6.17	48.68	1.74

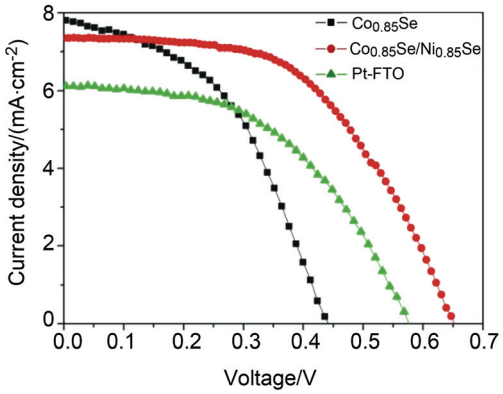

Figure 6 Characteristic photocurrent density-voltage (*J-V*) curves of DSSCs with different electrodes, measured under simulated sunlight 100 mW•cm^{-2} (AM 1.5). The liquid electrolyte is composed of 0.22 mol/L cobalt(II), 0.055 mol/L cobalt(III), 0.2 mol/L 4-*tert*-butylpyridine (TBP) and 0.1 mol/L LiTFSI in acetonitrile.

$Co_{0.85}Se$, which is different from reduction for the iodide/triiodide electrolyte.

As we know, electrochemical impedance spectroscopy (EIS) is an important method to study the reaction mechanism. Figure 7 shows the Nyquist plots of various CEs and Table 1 shows the impedance parameters of various CEs for cobalt complex redox couple. The R_s in cobalt(II/III) redox electrolyte showed the same discipline with that of I_3^-/I^- redox electrolyte for $Co_{0.85}Se$, $Co_{0.85}Se/Ni_{0.85}Se$ and Pt-FTO electrodes. The R_{ct} of $Co_{0.85}Se/Ni_{0.85}Se$ was merely 7.39 Ω•cm^2, much smaller than that of $Co_{0.85}Se$ (31.92 Ω•cm^2) and that of Pt-FTO (76.46 Ω•cm^2), suggesting a better electrocatalytic activity for the cobalt(II/III) redox couples in the $Co_{0.85}Se/Ni_{0.85}Se$ CEs. The regularities of three kinds of CEs are different between I_3^-/I^- electrolyte and Co(II/III) electrolyte. To investigate the mechanism of improved catalytic activty for Co(II/III) redox couple, nickel selenide was synthesized at the same condition with that of $Co_{0.85}Se/Ni_{0.85}Se$. However, it is unfortunate that Ni_3Se_2 rather than $Ni_{0.85}Se$ was obtained. The DSSCs using Ni_3Se_2 CEs for cobalt complex electrolyte showed PCEs of 0.2%. The R_{ct} of Ni_3Se_2 was very large and up to 300.03 Ω•cm^2. These results demonstrated the number of effective catalytic active sites for catalyst which possesses a low porosity and pore diameter may become less due to pore diameter limitation for cobalt redox couples. Therefore, we speculated that better catalytic activity of $Co_{0.85}Se/Ni_{0.85}Se$ for Co(II/III) redox couple may be attributed to synergistic effect and the unique

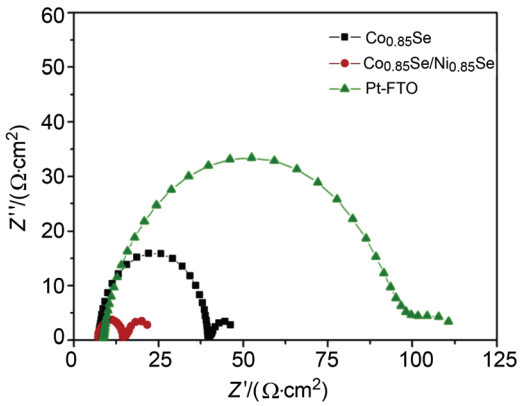

Figure 7 Nyquist plots for symmetric cells fabricated with two identical counter electrode of Pt, $Co_{0.85}Se$ and $Co_{0.85}Se/Ni_{0.85}Se$ filled with Co(II/III) electrolyte. The cells were measured in the frequency range between 100 kHz and 100 mHz.

morphology of nanoparticles embeded with 2D nanoflakes of $Co_{0.85}Se/Ni_{0.85}Se$, which supplied more catalytic activity for larger volume cobalt(II/III) redox couples than $Co_{0.85}Se$ nanosheets and Pt nanoparticles.

Conclusions

In summary, $Co_{0.85}Se/Ni_{0.85}Se$ nanocomposite films were electrochemically deposited on FTO glass at ambient temperature and used as CE catalysts in DSSCs for reduction of triiodide and Co(III). $Co_{0.85}Se/Ni_{0.85}Se$ nanocomposite counter electrode displayed comparable photovoltaic performance compared with a conventional Pt counter electrode and $Co_{0.85}Se$ counter electrode in I_3^-/I^- electrolyte. Moreover, it manifested better photovoltaic performance than Pt counter electrode and $Co_{0.85}Se$ counter electrode in Co(II)/Co(III) electrolyte. We believe that the current work paves the way for the design of nanostructured electro-catalyst for the reduction of larger volume Co(III) in DSSCs electrolyte.

Acknowledgement

This work was supported by the National Program on Key Basic Research Project of China (973 Program) (No. MOST2011CB935700), the National Natural Science Foundation of China (Nos. 21202178, 21271180), the Shandong Province Natural Science Foundation (Nos. ZR2011BQ024, ZR2013FZ001 and ZR2010BM016).

References

[1] O'Regan, B.; Grätzel, M. *Nature* **1991**, *353*, 737.
[2] Grätzel, M. *Nature* **2001**, *414*, 338.
[3] Peter, L. M. *Phys. Chem. Chem. Phys.* **2007**, *9*, 2630.
[4] Yang, N.; Zhai, J.; Wang, D.; Chen, Y.; Jiang, L. *ACS Nano* **2010**, *4*, 887.
[5] Wang, X.; Zhi, L.; Müellen, K. *Nano Lett.* **2008**, *8*, 323.
[6] Wang, J.; Lin, Z. *Chem.-Asian J.* **2012**, *7*, 2754.
[7] Peter, L. M. *Phys. Chem. Chem. Phys.* **2007**, *9*, 2630.
[8] Kang, T. S.; Chun, K. H.; Hong, J. S.; Moon, S. H.; Kim, K. J. *J. Electrochem. Soc.* **2000**, *147*, 3049.
[9] Nusbaumer, H.; Zakeeruddin, S. M.; Moser, J. E.; Grätzel, M. *Chemistry* **2003**, *9*, 3756.
[10] Wang, Q.; Ito, S.; Grätzel, M.; Fabregat-Santiago, F.; Mora-Sero, I.; Bisquert, J.; Bessho, T.; Imai, H. *J. Phys. Chem. B* **2006**, *110*, 25210.
[11] Snaith, H. J. *Adv. Funct. Mater.* **2010**, *20*, 13.
[12] Zhang, Z. *Adv. Funct. Mater.* **2008**, *18*, 341.
[13] Liu, Y.; Jennings, J. R.; Parameswaran, M.; Wang, Q. *Energy Environ. Sci.* **2010**, *4*, 564.
[14] Wang, M.; Chamberland, N.; Breau, L.; Moser, J. E.; Humphry-Baker, R.; Marsan, B.; Zakeeruddin, S. M.; Grätzel, M. *Nat. Chem.* **2010**, *2*, 385.
[15] Daeneke, T.; Kwon, T. H.; Holmes, A. B.; Duffy, N. W.; Bach, U.; Spiccia, L. *Nat. Chem.* **2011**, *3*, 213.
[16] Bai, Y.; Yu, Q.; Cai, N.; Wang, Y.; Zhang, M.; Wang, P. *Chem. Commun*. **2011**, *47*, 4376.
[17] Inamo, M.; Aoki, K.; Ono, N.; Takagi, H. D. *Inorg. Chem. Commun.* **2005**, *8*, 979.
[18] Hattori, S.; Wada, Y.; Yanagida, S.; Fukuzumi, S. *J. Am. Chem. Soc.* **2005**, *127*, 9648.
[19] Nusbaumer, H.; Moser, J.-E.; Zakeeruddin, S. M.; Nazeeruddin, M. K.; Grätzel, M. *J. Phys. Chem. B* **2001**, *105*, 10461.
[20] Sapp, S. A. *J. Am. Chem. Soc.* **2002**, *124*, 11215.
[21] Cameron, P.; Peter, L.; Zakeeruddin, S.; Grätzel, M. *Coord. Chem. Rev.* **2004**, *248*, 1447.
[22] Feldt, S. M.; Gibson, E. A.; Gabrielsson, E.; Sun, L.; Boschloo, G.; Hagfeldt, A. *J. Am. Chem. Soc.* **2010**, *132*, 16714.
[23] Gibson, E. A.; Smeigh, A. L.; Le Pleux, L. C.; Hammarström, L.; Odobel, F.; Boschloo, G.; Hagfeldt, A. *J. Phys. Chem. C* **2011**, *115*, 9772.
[24] Yella, A.; Lee, H.-W.; Tsao, H. N.; Yi, C.; Chandiran, A. K.; Khaja Nazeeruddin, M. D.; Diau, E. W.-G.; Yeh, C.-Y.; Zakeeruddin, S. M.; Grätzel, M. *Science* **2011**, *334*, 629.
[25] Wang, H.; Sun, K.; Tao, F.; Stacchiola, D. J.; Hu, Y. H. *Angew. Chem., Int. Ed.* **2013**, *52*, 9210.
[26] Wu, M.; Lin, X.; Wang, T.; Qiu, J.; Ma, T. *Energy Environ. Sci.* **2011**, *4*, 2308.
[27] Yang, Z.; Liu, M.; Zhang, C.; Tjiu, W. W.; Liu, T.; Peng, H. *Angew. Chem., Int. Ed.* **2013**, *52*, 3996.
[28] Wang, H.; Hu, Y. H. *Energy Environ. Sci.* **2012**, *5*, 8182.
[29] Wang, H.; Feng, Q.; Gong, F.; Li, Y.; Zhou, G.; Wang, Z.-S. *J. Mater. Chem. A* **2013**, *1*, 97.
[30] (a) Tai, Q.; Chen, B.; Guo, F.; Xu, S.; Hu, H.; Sebo, B.; Zhao, X.-Z.; *ACS Nano* **2011**, *5*, 3795; (b) Zhang, T.-L.; Chen, H.-Y.; Su, C.-Y.; Kuang, D.-B. *J. Mater. Chem. A* **2013**, *1*, 1724.
[31] Jiang, Q. W.; Li, G. R.; Gao, X. P. *Chem. Commun.* **2009**, 6720.
[32] Wu, M.; Zhang, Q.; Xiao, J.; Ma, C.; Lin, X.; Miao, C.; He, Y.; Gao, Y.; Hagfeldt, A.; Ma, T. *J. Mater. Chem.* **2011**, *21*, 10761.
[33] Zhang, X.; Chen, X.; Dong, S.; Liu, Z.; Zhou, X.; Yao, J.; Pang, S.; Xu, H.; Zhang, Z.; Li, L.; Cui, G. *J. Mater. Chem.* **2012**, *22*, 6067.
[34] Wu, M.; Lin, X.; Hagfeldt, A.; Ma, T. *Angew. Chem., Int. Ed.* **2011**, *50*, 3520.
[35] Wu, M.; Lin, X.; Wang, Y.; Wang, L.; Guo, W.; Qi, D.; Peng, X.; Hagfeldt, A.; Grätzel, M.; Ma, T. *J. Am. Chem. Soc.* **2012**, *134*, 3419.
[36] Wang, M.; Anghel, A. M.; Marsan, B.; Cevey Ha, N.-L.; Pootrakulchote, N.; Zakeeruddin, S. M.; Grätzel, M. *J. Am. Chem. Soc.* **2009**, *131*, 15976.
[37] Ku, Z.; Li, X.; Liu, G.; Wang, H.; Rong, Y.; Xu, M.; Liu, L.; Hu, M.; Yang, Y.; Han, H. *J. Mater. Chem. A* **2013**, *1*, 237.
[38] Kung, C.-W.; Chen, H.-W.; Lin, C.-Y.; Huang, K.-C.; Vittal, R.; Ho, K.-C. *ACS Nano* **2012**, *6*, 7016.
[39] Xin, X.; He, M.; Han, W.; Jung, J.; Lin, Z. *Angew. Chem., Int. Ed.* **2011**, *50*, 11739.
[40] Gong, F.; Wang, H.; Xu, X.; Zhou, G.; Wang, Z.-S. *J. Am. Chem.*

Soc. **2012**, *134*, 10953.
[41] (a) Zhang, Z.; Pang, S.; Xu, H.; Yang, Z.; Zhang, X.; Liu, Z.; Wang, Z.; Zhou, X.; Dong, S.; Chen, X.; Gu, L.; Cui, G. *RSC Adv.* **2013**, *3*, 16528; (b) Gong, F.; Xu, X.; Li, Z.; Zhou, G.; Wang, Z.-S. *Chem. Commun.* **2013**, *49*, 1437.
[42] Guo, J.; Shi, Y.; Chua, Y.; Ma, T. *Chem. Commun.* **2013**, *49*, 10157.
[43] Feldt, S. M.; Gibson, E. A.; Gabrielsson, E.; Sun, L. C.; Boschloo, G.; Hagfeldt, A. *J. Am. Chem. Soc.* **2010**, *132*, 16714.
[44] Popov, A. I.; Geske, D. H. *J. Am. Chem. Soc.* **1958**, *80*, 1340.
[45] Zhao, W.; Lin, T.; Sun, S.; Bi, H.; Chen, P.; Wan, D.; Huang, F. *J. Mater. Chem. A* **2013**, *1*, 194.
[46] Fabregat-Santiago, F.; Bisquert, J.; Palomares, E.; Otero, L.; Kuang, D.; Zakeeruddin, S. M.; Grätzel, M. *J. Phys. Chem. C* **2007**, *111*, 6550.

(Lu, Y.)

